Corroles

Deutsche Ausgabe: DOI: 10.1002/ange.201601864
Internationale Ausgabe: DOI: 10.1002/anie.201601864

Triply Linked Corrole Dimers

Shota Ooi, Takayuki Tanaka, Kyu Hyung Park, Dongho Kim,* and Atsuhiro Osuka**

Abstract: *The oxidation of 10–10′ singly linked corrole dimers with DDQ at low concentration in $CHCl_3$ afforded meso–meso, β–β, β–β triply linked 2H-corrole dimers (with two inner NH groups in each corrole unit), which exhibited characteristic ^1H NMR and absorption spectra attributable to their non-aromatic electronic networks. These 2H-corrole dimers were reduced with $NaBH_4$ to aromatic 3H-corrole dimers, which were unstable and easily oxidized back to the 2H-corrole dimers upon exposure to air. Bis(zinc(II)) complexes of the 2H-corrole dimers were synthesized and characterized as rare examples of nonaromatic zinc(II) corrole complexes.*

Direct triple linkages of porphyrinoids have been demonstrated to be the most effective means to obtain coplanar structures and strongly conjugated π-electronic networks. As a representative example, meso–meso, β–β, β–β triply linked porphyrin arrays were reported by our group in 2000.[1] Since then, these molecules have been extensively studied in light of their remarkably red-shifted absorption bands, large two-photon absorption cross-sections, multicharge acceptor properties, and high electroconductivity.[1,2] Aside from these structures, a variety of triply linked porphyrin derivatives, including anthracene-,[3a–c] BODIPY-,[3d] and diphenylamine-fused porphyrins,[3e] have been explored and display intriguing optical and electrochemical properties.[3] In general, triply linked porphyrin dimers **2** are effectively synthesized by the oxidation of singly linked dimers **1** with 2,3-dichloro-5,6-dicyano-1,4-benzoquinone (DDQ) and $Sc(OTf)_3$ (Scheme 1).[1b–f,2c–e] This method has recently been applied to obtain hybrid tape **4** from the porphyrin–hexaphyrin hybrid dimer **3**.[4]

Corrole is a congener of porphyrin with one less carbon atom but its chemistry is distinctly different from that of porphyrin. In particular, corroles allow for the formation of various high-valent metal complexes owing to their narrower pocket and three inner pyrrolic protons. The chemistry of corroles experienced an upsurge of interest when the groups of Gross, Gryko, and Paolesse independently reported improved syntheses of 5,10,15-triaryl-substituted corroles.[5] Despite this progress, the chemistry of directly linked corrole oligomers has rarely been studied compared to the porphyrin counterpart. Singly linked oligomers were synthesized by Gross and co-workers and our group,[6] and later, the doubly 2,18-linked dimer **5**[7] and the doubly 3,5-linked dimer **6**[8] were synthesized from the corresponding singly linked dimers through an oxidative fusion reaction with DDQ. Interestingly, dimer **5** exists as a stable open-shell singlet biradicaloid molecule, whereas the stable form of **6** is an unusual 2*H*-corrole, a closed-shell, nonaromatic molecule with a partially helicene-like structure.

A meso–meso, β–β, β–β triply linked corrole dimer could be a milestone molecule, and its synthesis was already envisioned by Gryko and Koszarna in 2007.[9] They attempted

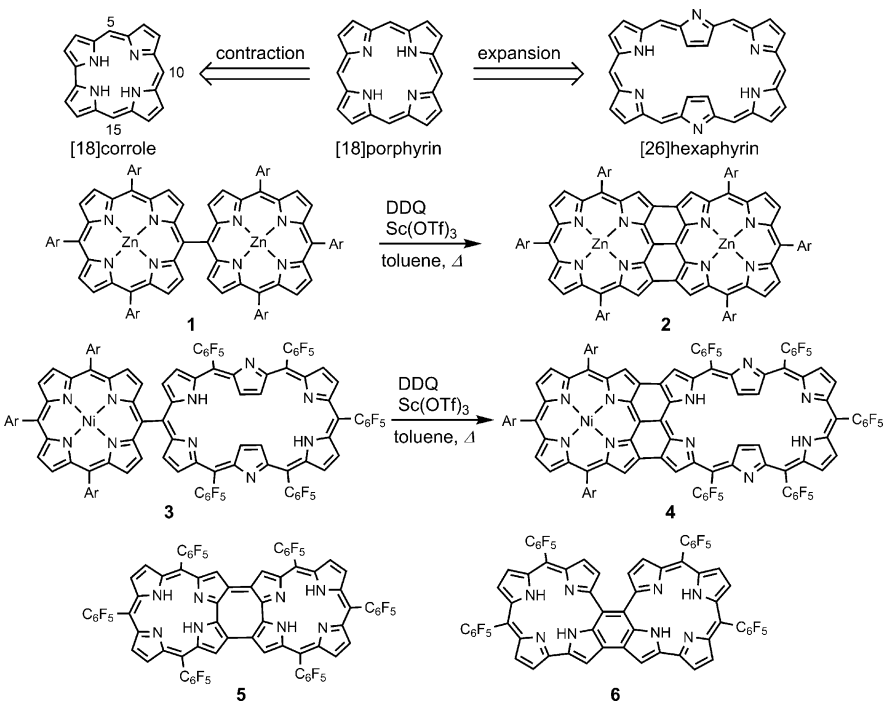

Scheme 1. Porphyrin tapes (**2**), porphyrin–hexaphyrin hybrid tapes (**4**), and fused corrole dimers (**5** and **6**).

[*] S. Ooi, Dr. T. Tanaka, Prof. Dr. A. Osuka
Department of Chemistry, Graduate School of Science
Kyoto University
Sakyo-ku, Kyoto 606-8502 (Japan)
E-mail: taka@kuchem.kyoto-u.ac.jp
osuka@kuchem.kyoto-u.ac.jp
K. H. Park, Prof. Dr. D. Kim
Spectroscopy Laboratory for Functional π-Electronic Systems and
Department of Chemistry
Yonsei University, Seoul 120-749 (Korea)
E-mail: dongho@yonsei.ac.kr

Supporting information for this article can be found under: http://dx.doi.org/10.1002/anie.201601864.

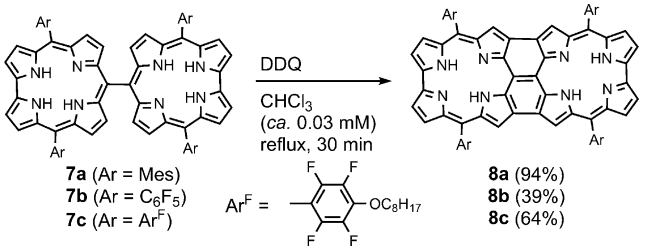

Scheme 2. Synthesis of triply linked corrole dimers.

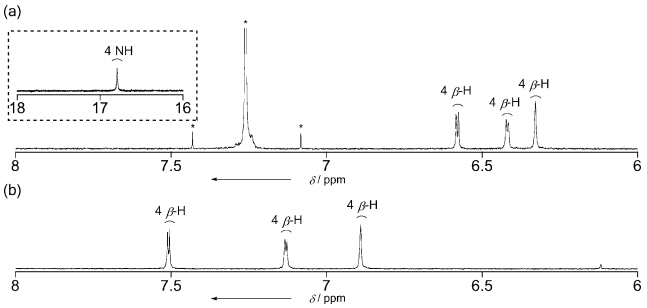

Figure 1. ^{1}H NMR spectra of a) **8c** in $CDCl_3$ and b) **9c** in [D_6]acetone with $NaBH_4$ at room temperature. Only the aromatic regions are shown. Peaks marked with * are due to the solvent.

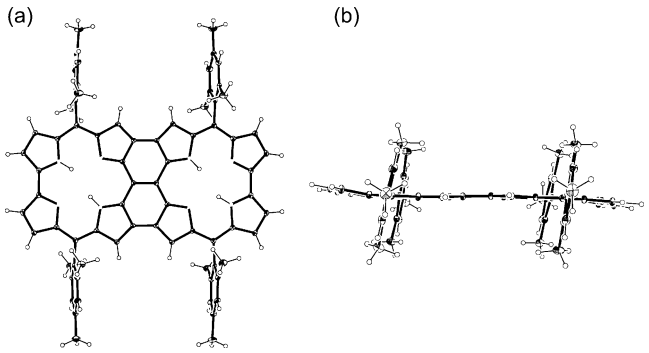

Figure 2. X-ray crystal structure of **8a**. a) Top view and b) side view. Thermal ellipsoids set at 30% probability. Solvent molecules were omitted for clarity.

to oxidize the 10,10′-linked corrole dimer **7a** with DDQ and $Sc(OTf)_3$ but did not obtain the desired product because of oxidative decomposition (Scheme 2). Recently, we synthesized the 10,10′-linked dimer **7b**, which bears four electron-withdrawing pentafluorophenyl substituents, by oxidative meso–meso coupling of meso-free corrole.[10] It occurred to us that **7b** would be more robust towards oxidative degradation than **7a**. We thus attempted an intramolecular oxidative fusion reaction of **7b** with DDQ. We found that highly dilute conditions (ca. 0.03 mM) were required to avoid undesirable intermolecular oxidative couplings, and the oxidation of **7b** with DDQ (3.5 equiv) in $CHCl_3$ at reflux gave the triply linked corrole dimer **8b** in 39% yield as a dark pinkish solid (Scheme 2). High-resolution atmospheric-pressure chemical ionization time-of-flight mass spectrometry (APCI-TOF-MS) revealed a parent ion peak of **8b** at $m/z = 1252.1128$ (m/z calcd for $C_{62}H_{16}F_{20}N_8$: 1252.1179 $[M]^-$), indicating the loss of six hydrogen atoms from **7b** and thus a 2*H*-type oxidation state of the corrole ligand similar to those of **5** and **6**. The ^{1}H NMR spectrum of **8b** displayed two doublets at 6.63 and 6.43 ppm and one singlet at 6.32 ppm, which are due to the pyrrolic β-protons and indicate its nonaromatic nature (see the Supporting Information, Figure S3-3). A resonance that is due to pyrrolic NH protons was observed at 16.73 ppm. The large downfield shift of the NH resonance can be explained by intramolecular hydrogen-bonding interactions. Interestingly, **8b** is chemically fairly stable. As the solubility of **8b** was not very good, we prepared the more soluble 4-octyloxy-2,3,5,6-tetrafluorophenyl-substituted corrole dimer **7c**, and its oxidation under the same conditions afforded the fused dimer **8c** in 64% yield (for its ^{1}H NMR spectrum, see Figure 1a). Encouraged by these results, we retried the oxidation of **7a** under our optimized conditions, which, to our surprise, afforded the fused dimer **8a** in 94% yield. Importantly, the yield of **8a** decreased at higher concentrations (see the Supporting Information).

Fortunately, single crystals of **8a** suitable for X-ray diffraction analysis were obtained by slow vapor diffusion of *n*-heptane into a chloroform solution of **8a**. The structure of **8a** is depicted in Figure 2; the two corrole moieties are triply connected at the 8,8′, 10,10′, and 12,12′ positions with C–C bond lengths of 1.395(4), 1.389(4), and 1.395(4) Å, respectively.[11] Characteristically, these bonds are clearly shorter than those in **2** (1.43 and 1.48 Å),[12] implying that they have significant double-bond character. The two 2*H*-corrole moieties are highly coplanar with a mean plane deviation of 0.051 Å as a result of the direct triple linkage.[13] In spite of the nonaromatic nature of this compound, a bond-length alternation could not be clearly observed. A crystal structure of **7a** was also obtained (Figure S5-1). The central C10–C10′ bond length is 1.51(1)-1.52(1) Å, and the two corrole mean planes are almost orthogonal to each other (dihedral angle: 86.2–88.8°), indicating that the electronic interactions between the two corroles are almost negligible.

The fused dimer **8a** exhibits split Soret-like bands at 520 and 546 nm and a broad band at 653 nm along with a weak absorption tail extending into the NIR region in CH_2Cl_2 (Figure 3a). The absorbance of **8a** is distinctly weaker than that of the 10–10′ linked corrole dimer **7a**, presumably as a consequence of its nonaromatic nature. The absorption spectra of **8b** and **8c** are essentially similar to that of **8a**. DFT molecular-orbital calculations revealed that the orbital coefficients in the HOMO and LUMO are fully delocalized over the whole molecule. Furthermore, TD-DFT calculations reproduced the absorption spectrum (Figure S8-7). Therefore, the red-shifted absorptions of **8a**–**8c** could be assigned to transitions between the fully conjugated electronic states.

Cyclic voltammetry and differential pulse voltammetry experiments revealed reversible first and second oxidation waves at 0.30 and 0.57 V, and reversible first and second reduction waves at −0.79 and −1.07 V for **8a**, whereas **7a** displays irreversible first oxidation and reduction waves at 0.00 and −1.81 V, respectively, against the ferrocene/ferrocenium couple in benzonitrile (Table S2).[14] The electrochemical HOMO–LUMO gaps (ΔE_{HL}) were thus calculated to be

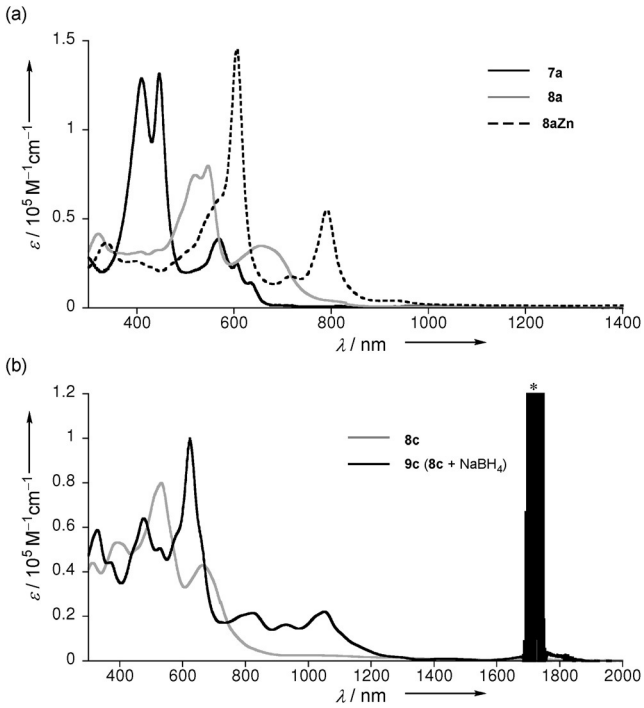

Figure 3. UV/Vis absorption spectra of a) **7a** and **8a** in CH_2Cl_2 and **8aZn** in THF and b) **8c** and **9c** (**8c** + $NaBH_4$) in THF. Peaks marked with * are due to solvent.

1.09 eV for **8a** and 1.81 eV for **7a**. The oxidation and reduction potentials of **8b** and **8c** are positively shifted by 0.1–0.2 V, reflecting the electron-withdrawing nature of the substituents. The ΔE_{HL} values of **8b** (0.98 eV) and **8c** (1.01 eV) are slightly smaller than that of **8a**.

We expected that reduction of the 2*H*-fused dimers **8** with $NaBH_4$ could afford the corresponding 3*H*-fused dimers **9**, which consist of two aromatic corroles as observed in the case of **6** (Scheme 3). Indeed, reduction of **8a** with $NaBH_4$ in THF/MeOH proceeded smoothly to give **9a**, which, however, quite easily reverted back to **8a** under aerobic conditions. The lower reduction potential of **8c** compared to that of **8a** enabled the detection of in situ generated reduced **9c** by ^1H and ^{19}F NMR spectroscopy in the presence of $NaBH_4$ (Figure 1b). The ^1H NMR spectrum of **9c** showed two doublets at 7.51 ($J = 3.4$ Hz) and 7.13 ppm ($J = 3.4$ Hz) and one singlet signal at 6.89 ppm, which are due to the β-protons, indicating the recovery of moderate aromaticity. On the basis of DFT calculations, the energy-minimized structures of **8** and **9** were predicted (see the Supporting Information). Accordingly, **9a** adopts an almost coplanar structure with a mean-plane deviation of 0.109 Å. The nucleus-independent chemical shift (NICS) values at the center of the 2*H*- and 3*H*-corrole rings are +4.95 ppm in **8a** and −5.43 ppm in **9a**, which is in accordance with the above assignments.[15] The dimer **9c** could also be detected by UV/Vis absorption spectroscopy, which revealed large split Soret-like bands at 472 and 623 nm and Q-like bands around 1000 nm (Figure 3b).

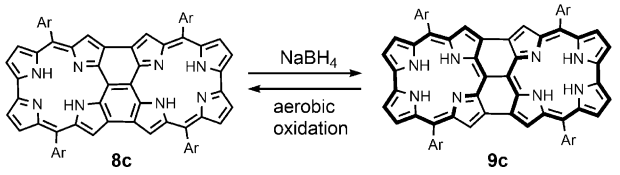

Scheme 3. Formation of **9c** by reduction of **8c**.

Finally, the metalation of **8a** with zinc(II) as an exemplary divalent metal was attempted. The reaction of **8a** with $Zn(OAc)_2{\cdot}2H_2O$ in $CHCl_3$ at reflux for 20 h gave Zn^{II} complex **8aZn** in 76% yield (Scheme 4). High-resolution electrospray ionization time-of-flight mass spectrometry (ESI-TOF-MS) of **8aZn** revealed its parent ion peak at $m/z = 1188.3191$ (calcd for $C_{74}H_{56}N_8{}^{64}Zn_2$: 1188.3165 $[M]^+$). Under similar conditions, more soluble **8c** was also metalated to give **8cZn** in 79% yield. We also attempted the nickelation of **8a**–**8c** using $Ni(acac)_2$ but failed, probably owing to the mismatching coordination mode of Ni^{II}. The ^1H NMR spectrum of complex **8aZn** in [D_5]pyridine displays two doublets at 6.17 and 6.06 ppm and a singlet at 5.42 ppm, which are due to the pyrrolic protons, along with signals that are due to the mesityl group, again confirming its nonaromatic nature. The structure of **8aZn** was revealed by X-ray diffraction analysis of a single crystal of **8aZn** grown in the presence of *n*-butylamine (Figure 4).[16] Complex **8aZn** shows five-coordinate square-pyramidal coordination. The Zn^{II} center is displaced out of the corrole N_4 plane by 0.579 Å, and the whole structure is slightly bowl-shaped. Owing to its poor solubility, the solid-state structure without any coordinating ligands on the Zn atoms could not been obtained. Instead, DFT calculations of **8aZn** without any amine coordination predicted its optimized structure to be a slightly more planar structure with a Zn^{II} displacement of approximately 0.289 Å.

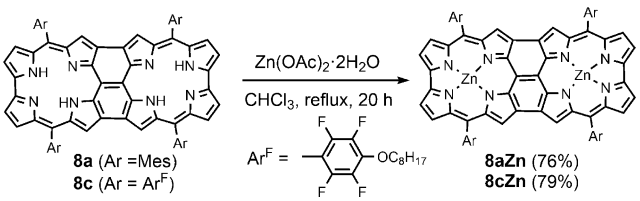

Scheme 4. Metalation of **8a** and **8c** with zinc(II).

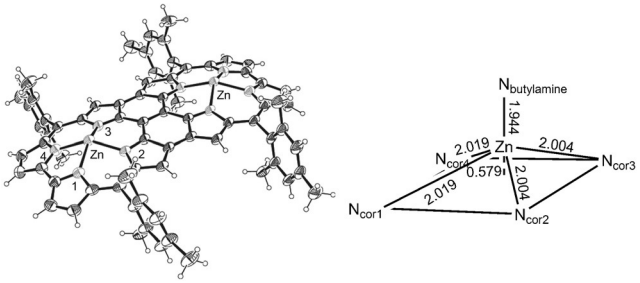

Figure 4. X-ray crystal structure of **8aZn**. Thermal ellipsoids set at 30% probability. *n*-Butylamine ligands coordinated to the Zn atoms and solvent molecules were omitted for clarity. Bond lengths are given in Å.

Complex **8aZn** exhibits sharper and more red-shifted absorption bands than **8a** (Figure 3a). Cyclic voltammetry measurements of **8aZn** revealed the first and second oxidation potentials at −0.13 and 0.24 V and the first and second reduction potentials as reversible waves at −0.97 and −1.39 V. The ΔE_{HL} value was thus calculated to be 0.84 eV.

To investigate the excited-state dynamics of these corrole dimers, we measured their transient absorption (TA) spectra. The TA spectra of **7a**–**7c** exhibited intense negative bands around 460 nm and from 570 to 670 nm, which correspond to ground-state bleaching (GSB) of a lower-energy split Soret band and Q-bands, respectively (Figure S9-1). The stimulated emission (SE) signals of **7a**–**7c**, which overlap with the GSB signal from 620 to 670 nm, rapidly decayed within 300 ps owing to the red shift of the SE, which originates from the structural relaxation along the intercorrole torsion angle, as previously reported for 5,5′-linked corrole dimers.[8a] The decay dynamics of GSB show a biexponential decay with the fast component ($\tau_1 = 90$ ps for **7a** and 26 ps for **7c**) matching the torsional relaxation time of meso–meso linked porphyrin dimers.[17] On the other hand, **8a**–**8c** exhibited ultrafast triexponential decay owing to increased electronic interactions as a result of the fusion of the two corrole units (Figure S9-2). The initial picosecond decay ($\tau_1 = 1.2$ ps for **8a** and 0.8 ps for **8c**) can be explained by internal conversion to the dark state, and the subsequent decay ($\tau_2 = 12$ ps for **8a** and 7.7 ps for **8c**) can be explained by vibrational cooling, a process often observed for fused diporphyrins.[18] Ground-state recovery showed lifetimes of 220 ps for **8a** and 100 ps for **8c**, which are significantly shorter than that of a corrole monomer ($\tau_{fl} = 4.87$ ns), which is primarily due to the reduced HOMO–LUMO gap. The reduction of **8c** with $NaBH_4$ led to the recovery of aromaticity as inferred from the fourfold increase in the excited-state lifetime, $\tau_3 = 450$ ps for **9c**, which is consistent with the ^{1}H NMR spectra (Figure S9-3). Zincation of **8a** and **8c** was shown to greatly alter the excited-state dynamics of the triply linked corroles. Unlike **8a**–**8c**, **8aZn** and **8cZn** are completely depopulated within 40 ps (Figure S9-4). The GSB decays can be analyzed in terms of biexponential decay functions, with $\tau_1 = 1.6$ ps and $\tau_2 = 12$ ps for **8aZn** and $\tau_1 = 1.5$ ps and $\tau_2 = 11$ ps for **8cZn**. The initial decay within picoseconds presumably indicates internal conversion to the lowest-energy state in the near-IR region as well as vibrational energy redistribution processes. Subsequent internal conversion to the ground state exhibits time constants that are rather similar to those reported for free-base and metalated fused diporphyrins.[19] Although dramatic reductions of the singlet excited-state lifetimes upon zinc insertion have been reported for various porphyrinoids,[20] we suggest that in the present case, the doming distortion induced by the zinc atom at the core of each corrole unit leads to an enhancement of nonradiative deactivation processes, as previously reported in the study of nonplanar porphyrins.[20]

In summary, the meso–meso, β–β, β–β triply linked corrole dimers **8a**–**8c** have been synthesized as stable entities for the first time by oxidation of the meso–meso singly linked corrole dimers **7a**–**7c** with DDQ at low concentration. The triply linked structures were confirmed by X-ray analysis. The dimers **8a**–**8c** were determined to be nonaromatic 2*H*-corroles by ^{1}H NMR and absorption spectroscopy. The dimer **8c** was reduced with $NaBH_4$ to give the aromatic 3*H*-corrole dimer **9c**, which showed ^{1}H NMR and UV/Vis absorption spectra that are in accordance with its moderate aromatic character. The unusual properties of these triply linked corrole dimers may be ascribed to the direct triple linkage between the two corroles. We are currently pursuing further functional systems based on corroles with multiple direct linkages in our laboratory.

Acknowledgements

The work at Kyoto was supported by JSPS KAKENHI Grants (25220802 and 25620031). The work at Yonsei was supported by the Global Research Laboratory (GRL) Program funded by the Ministry of Science, ICT & Future, Korea (2013K1A1A2A02050183).

Keywords: aromaticity · conjugation · corroles · oxidation · porphyrinoids

How to cite: *Angew. Chem. Int. Ed.* **2016**, *55*, 6535–6539
Angew. Chem. **2016**, *128*, 6645–6649

[1] a) A. Tsuda, H. Furuta, A. Osuka, *Angew. Chem. Int. Ed.* **2000**, *39*, 2549; *Angew. Chem.* **2000**, *112*, 2649; b) A. Tsuda, A. Osuka, *Science* **2001**, *293*, 79; c) D. Bonifazi, M. Sholl, F. Song, L. Echegoyen, G. Accorsi, N. Armaroli, F. Diederich, *Angew. Chem. Int. Ed.* **2003**, *42*, 4966; *Angew. Chem.* **2003**, *115*, 5116; d) Y. Nakamura, S. Y. Jang, T. Tanaka, N. Aratani, J. M. Lim, K. S. Kim, D. Kim, A. Osuka, *Chem. Eur. J.* **2008**, *14*, 8279; e) T. Ikeda, N. Aratani, A. Osuka, *Chem. Asian J.* **2009**, *4*, 1248; f) T. Tanaka, B. S. Lee, N. Aratani, M.-C. Yoon, D. Kim, A. Osuka, *Chem. Eur. J.* **2011**, *17*, 14400; g) G. Sedghi, V. M. García-Suárez, L. J. Esdaile, H. L. Anderson, C. J. Lambert, S. Martin, D. Bethell, S. J. Higgins, M. Elliott, N. Bennett, J. E. Macdonald, R. J. Nichols, *Nat. Nanotechnol.* **2011**, *6*, 517; h) G. Sedghi, L. J. Esdaile, H. L. Anderson, S. Martin, D. Bethell, S. J. Higgins, R. J. Nichols, *Adv. Mater.* **2012**, *24*, 653.

[2] a) N. Aratani, D. Kim, A. Osuka, *Chem. Asian J.* **2009**, *4*, 1172; b) J. P. Lewtak, D. T. Gryko, *Chem. Commun.* **2012**, *48*, 10069; c) H. Mori, T. Tanaka, A. Osuka, *J. Mater. Chem. C* **2013**, *1*, 2500; d) M. Grzybowski, K. Skonieczny, H. Butenschön, D. T. Gryko, *Angew. Chem. Int. Ed.* **2013**, *52*, 9900; *Angew. Chem.* **2013**, *125*, 10084; e) T. Tanaka, A. Osuka, *Chem. Soc. Rev.* **2015**, *44*, 943.

[3] a) I. M. Blake, A. Krivokapic, M. Ketterle, H. L. Anderson, *Chem. Commun.* **2002**, 1662; b) N. K. S. Davis, M. Pawlicki, H. L. Anderson, *Org. Lett.* **2008**, *10*, 3945; c) N. K. S. Davis, A. L. Thompson, H. L. Anderson, *J. Am. Chem. Soc.* **2011**, *133*, 30; d) C. Jiao, L. Zhu, J. Wu, *Chem. Eur. J.* **2011**, *17*, 6610; e) N. Fukui, W.-Y. Cha, S. Lee, S. Tokuji, D. Kim, H. Yorimitsu, A. Osuka, *Angew. Chem. Int. Ed.* **2013**, *52*, 9728; *Angew. Chem.* **2013**, *125*, 9910.

[4] a) T. Tanaka, N. Aratani, J. M. Lim, K. S. Kim, D. Kim, A. Osuka, *Chem. Sci.* **2011**, *2*, 1414; b) T. Tanaka, A. Aratani, A. Osuka, *Chem. Asian J.* **2012**, *7*, 889; c) H. Mori, T. Tanaka, S. Lee, J. M. Lim, D. Kim, A. Osuka, *J. Am. Chem. Soc.* **2015**, *137*, 2097.

[5] a) Z. Gross, N. Galili, I. Saltsman, *Angew. Chem. Int. Ed.* **1999**, *38*, 1427; *Angew. Chem.* **1999**, *111*, 1530; b) R. Paolesse, L. Jaquinod, D. J. Nurco, S. Mini, F. Sagone, T. Boschia, K. M. Smith, *Chem. Commun.* **1999**, 1307; c) D. T. Gryko, *Chem. Commun.* **2000**, 2243; d) D. T. Gryko, *Eur. J. Org. Chem.* **2002**,

1735; e) R. Paolesse, A. Marini, S. Nardis, A. Froiio, F. Mandoj, D. J. Nurco, L. Prodi, M. Montalti, K. M. Smith, *J. Porphyrins Phthalocyanines* **2003**, *7*, 25; f) D. T. Gryko, J. P. Fox, D. P. Goldberg, *J. Porphyrins Phthalocyanines* **2004**, *8*, 1091; g) Z. Gross, H. B. Gray, *Adv. Synth. Catal.* **2004**, *346*, 165; h) I. Aviv, Z. Gross, *Chem. Commun.* **2007**, 1987; i) R. Paolesse, *Synlett* **2008**, 2215; j) D. T. Gryko, *J. Porphyrins Phthalocyanines* **2008**, *12*, 906; k) I. Aviv-Harel, Z. Gross, *Chem. Eur. J.* **2009**, *15*, 8382; l) J. L. Flamigni, D. T. Gryko, *Chem. Soc. Rev.* **2009**, *38*, 1635.

[6] a) A. Mahammed, I. Giladi, I. Goldberg, Z. Gross, *Chem. Eur. J.* **2001**, *7*, 4259; b) I. Luobeznova, L. Simkhovich, I. Goldberg, Z. Gross, *Eur. J. Inorg. Chem.* **2004**, 1724; c) T. H. Ngo, W. V. Rossom, W. Dehaen, W. Maes, *Org. Biomol. Chem.* **2009**, *7*, 439; d) S. Hirabayashi, M. Omote, N. Aratani, A. Osuka, *Bull. Chem. Soc. Jpn.* **2012**, *85*, 558.

[7] a) S. Hiroto, I. Hisaki, H. Shinokubo, A. Osuka, *Angew. Chem. Int. Ed.* **2005**, *44*, 6763; *Angew. Chem.* **2005**, *117*, 6921; b) S. Hiroto, K. Furukawa, H. Shinokubo, A. Osuka, *J. Am. Chem. Soc.* **2006**, *128*, 12380.

[8] a) S. Ooi, T. Tanaka, K. H. Park, S. Lee, D. Kim, A. Osuka, *Angew. Chem. Int. Ed.* **2015**, *54*, 3107; *Angew. Chem.* **2015**, *127*, 3150; b) S. Ooi, T. Tanaka, A. Osuka, *Eur. J. Org. Chem.* **2015**, 130.

[9] B. Koszarna, D. T. Gryko, *Chem. Commun.* **2007**, 2994.

[10] S. Ooi, T. Yoneda, T. Tanaka, A. Osuka, *Chem. Eur. J.* **2015**, *21*, 7772.

[11] Crystallographic data for **8a**: $C_{78}H_{64}Cl_{12}N_8$, $M_r = 1538.77$, monoclinic, space group $P2_1/c$ (No. 14), $a = 17.986(3)$, $b = 12.2841(16)$, $c = 18.300(3)$ Å, $\beta = 118.021(2)°$, $V = 3569.3(10)$ Å^3, $Z = 2$, $R1 = 0.0505$ ($I > 2\sigma(I)$), $R_w = 0.1486$ (all data), GOF = 1.049. CCDC 1454202.

[12] T. Tanaka, Y. Nakamura, A. Osuka, *Chem. Eur. J.* **2008**, *14*, 204.

[13] Mean-plane deviations were calculated by considering the average distances between the corrole mean plane (the 23 core atoms) and each atom.

[14] J. Shen, J. Shao, Z. Ou, W. E, B. Koszarna, D. T. Gryko, K. M. Kadish, *Inorg. Chem.* **2006**, *45*, 2251.

[15] a) P. v. R. Schleyer, C. Maerker, A. Dransfeld, H. Jiao, N. J. R. van Eikema Hommes, *J. Am. Chem. Soc.* **1996**, *118*, 6317; b) Z. Chen, C. S. Wannere, C. Corminboeuf, R. Puchta, P. v. R. Schleyer, *Chem. Rev.* **2005**, *105*, 3842.

[16] Crystallographic data for **8aZn**: $C_{230}H_{112}N_{20}O_{12}Zn_4$, $M_r = 3608.96$, orthorhombic, space group *Fmmm* (No. 69), $a = 30.000(7)$, $b = 22.846(5)$, $c = 31.625(13)$ Å, $V = 21675(11)$ Å^3, $Z = 4$, $R1 = 0.0813$ ($I > 2\sigma(I)$), $R_w = 0.2818$ (all data), GOF = 1.076. CCDC 1454203.

[17] M. U. Winters, J. Kärnbratt, M. Eng, C. J. Wilson, H. L. Anderson, B. Albinsson, *J. Phys. Chem. C* **2007**, *111*, 7192.

[18] H. S. Cho, D. H. Jeong, S. Cho, D. Kim, Y. Matsuzaki, K. Tanaka, A. Tsuda, A. Osuka, *J. Am. Chem. Soc.* **2002**, *124*, 14642.

[19] D. Y. Kim, T. K. Ahn, J. H. Kwon, D. Kim, T. Ikeue, N. Aratani, A. Osuka, M. Shigeiwa, S. Maeda, *J. Phys. Chem. A* **2005**, *109*, 2996.

[20] S. Gentemann, N. Y. Nelson, L. Jaquinod, D. J. Nurco, S. H. Leung, C. J. Medforth, K. M. Smith, J. Fajer, D. Holten, *J. Phys. Chem. B* **1997**, *101*, 1247.

Received: February 23, 2016
Published online: April 1, 2016

